Modeling of Nickel Hydroxide Electrode Containing Multiple Phases

P. Timmerman, B. V. Ratnakumar, and S. Di Stefano
Jet Propulsion Laboratory
California Institute of Technology
4800 Oak Grove Dr., Pasadena, CA 911 (W

ABSTRACT

Mathematical models of alkaline rechargeable nickel ccl] systems (e.g., Ni-Cd, Ni-112 and Ni-MH) have so far been developed based on the assumption that the active material at Ni electrode exists primarily in a single phase as β-NiOOH - β-Ni(OH)$_2$, despite enough experimental evidence for the second phase, i.e., γ-NiOOH - α-Ni(OH)$_2$, especially under conditions of extended overcharge. Here, we have incorporated the additional couple of γ-NiOOH - α-Ni(OH)$_2$ into the modeling, of the Ni electrode. The reaction scheme includes an electrochemical redox reaction of β-Ni(OH)$_2$ - β-NiOOH, unidirectional conversion of β-NiOOH to γ-NiOOH, electrochemical redox reaction α-Ni(OH)$_2$ - γ-NiOOH and a chemical conversion of α-Ni(OH)$_2$ to β-Ni(OH)$_2$. Changes in the electronic conductivities, proton concentrations, and the states of charge are monitored individually and coupled appropriately to obtain the response of the nickel electrode under variety of simulated test conditions. The multi-phase model has provided simulations of Ni electrode behavior with improved accuracy and agreement with the experimental data.

INTRODUCTION

Mathematical models would be greatly helpful in predicting the performance of batteries and providing guidelines for a proper management of power subsystem on spacecraft. In spacecraft, nickel-based rechargeable batteries are being used almost exclusively. JPL has been involved for the past few years in the development of first-principles mathematical models for aerospace, sealed Ni-Cd and Ni-112 rechargeable batteries. The earlier versions of these models were built around the cell models developed by White et al,[1-4] utilizing, the macrohomogeneous approach of Newman[5] for a description of porous electrodes. The more recent battery models at JPL, utilize relatively simplified treatments with respect to mass transport processes in electrolyte. Realizing that the concentration changes in liquid phase are relatively less prominent compared to gradients in solid phase (electrodes), the porous electrode treatment has been simplified

assuming a planar electrode geometry, with a homogeneous reaction on the electrode. Under these conditions. a semi-analytical solution can be obtained for the diffusion of protons across the positive active material layer.[6] This modification has resulted in considerable simplification with respect to computational needs, enabling them to be operational on portable computers. Furthermore, the predictions from the simplified model are generally consistent with the results from the complex porous electrode models, except at very high rates of discharge, where the mass transport processes in liquid phase should be treated more thoroughly. This approach is the basis of the current work, and has allowed an extensive modeling of' Ni electrode model by incorporating a treatment of multiple phases of active material.

REACTION SCHEME

Our earlier studies on the Ni-Cd boiler plate cell,[7] indicate that the shape of discharge curve changes appreciably on cycling. The discharge profiles in the beginning of cycling are rather flat, whereas those after cycling are distinctly sloping. The sloping nature of cycled Ni oxide electrode may be explained by a possible generation of a different phase of nickel oxyhydroxide during extensive cycling and/or overcharge. Nickel hydroxide or oxyhydroxide exists in multiple phases, i.e., α and β forms of $Ni(OH)_2$ and β and γ- forms of NiOOH.[8] In the normal course of cycling, β-$Ni(OH)_2$ gets converted to β-NiOOH on charge and vice versa on discharge. On prolonged charging or on overcharge, β-NiOOH is converted to γ-NiOOH. A larger number of electrons (about 1.5- 1,75) are exchanged per Ni atom during the α<>γ redox cycling. However, α-$Ni(OH)_2$ is unstable and transforms to its β-analogue on stand. Delahaye-Vidal et al.[9] suggested that α-$Ni(OH)_2$ contains the same sheets of $Ni(OH)_2$ in the lattice as the β-from, but in a disoriented manner along the c axis (hence termed as turbostratic) and with larger interlamellar spacing due to incorporation of electrolyte species. Furthermore, the α-form converts by dissolution- precipitation mechanism into thin platelets of β-$Ni(OH)_2$, which eventually grow to the usual thick platelets, The reversible potentials of these two phases are not known accurately, though et-y couple has reportedly a lower potential than the β-β couple.[10,11] Values of 0.39 and 0.44 V vs. Hg/HgO for the reversible potentials of α-γ and β-β couples, respectively, have been reported.[12] '1'0 add to this complexity, considerable hysteresis of 60- j 00 mV has been reported between oxidation and reduction potentials.[8]

In the incorporation of the above multiple phases of active material at Ni electrode, we have employed a similar reaction scheme. Accordingly, two phases of NiOOH/$Ni(OH)_2$ react independently as

$$\beta - NiOOH + H_2O + e^- <> \beta - Ni(OH)_2 + OH \qquad (1,)$$

$$\gamma - NiOOH + 1.5H_2O + 1.5e^- \leftrightarrow \gamma - Ni(OH)_2 + 1.5OH^- \quad (2.)$$

In addition, β-NiOOH is converted to γ-NiOOH upon overcharge (electrochemically) as:

$$\beta - NiOOH + 0.5e^- \Rightarrow \gamma - NiOOH \quad (3.)$$

It should be noted that the above reaction is irreversible. The conversion of β-NiOOH to γ-NiOOH involves co-intercalation o f electrolyte species into the lattice of γ-NiOOH, but is not included in this treatment.

Finally, α-$Ni(OH)_2$ undergoes a chemical transformation into a more stable β-$Ni(OH)_2$ by Ostwald's ripening, i.e., a morphological transition from thin platelets to thick plates by dissolution - precipitati on process;

$$\alpha - Ni(OH)_2 \Rightarrow \beta - Ni(OH)_2 \quad (4.)$$

Apart from the above reactions, there are several parasitic reactions involving electrolyte. For example, oxygen evolution occurs during charge and during self-discharge at the Ni electrode as:

$$O_2 + 4e^- + 2H_2O \leftrightarrow 4OH^- \quad (5.)$$

The above reaction is assumed to occur independently, similar to the reactions (1) and (2), at α-$Ni(OH)_2$ and β-$Ni(OH)_2$. Recombination of oxygen, which is a reverse of the above reaction occurs at the negative electrode, either Cd, H_2(for the present case of Ni-H_2 model), or metal hydride, along with the main reaction :

$$H_2 + 2OH^- \leftrightarrow 2H_2O + 2e^- \quad (6.)$$

The self-discharge of Ni electrode induced by hydrogen is similar to the cell discharge reactions, except that both the reactions occur on the positive electrode.

MODEL IMPLEMENTATION

In order to compute cell current (or potential) on applying a potential (current) perturbation, a set of differential equations have been formulated based on the application of principles of mass balance for each of the species in the above reactions, current balance, energy balance, mass transport, thermodynamics, and kinetics. In this model, the mass transport of protons through solid phase is treated by a semi-analytical solution

of Fick's second law.[6] The resulting solution requires the numerical solution of an integral for determining the proton diffusion gradients. The primary equations are solved using a Gaussian elimination method.

Proton Diffusion

It has been long realized that slow diffusion of protons in the lattice of the positive electrode material might contribute to mass transfer polarization which in turn affects the utilization of the positive electrode at high discharge rates. Proton concentration in the Ni oxide is calculated by solving, Fick's second law as:[6]

$$C(x,\tau) = \frac{1}{D(1-\Theta)} \int_0^{\tau} \left[1 + 2\sum_{k=1}^{\infty} (-1)^k e^{-k^2\pi^2(\tau - z)} \cos(k\pi x)\right] I(Z)\, dZ \qquad (7.)$$

where τ is the lime and x is the distance in dimensionless form. Proton concentration is thus monitored in the α-γ and β-β phases independently.

Electronic Conductivity of the Active Material

The conductivity of the positive electrode is a strong function of the slate of charge of the electrode; the conductivity of reduced phase is orders of magnitude lower than the conductivity of oxidized phase[13]. A modified empirical expression, similar to that used in the nickel-hydrogen model[13] is used to define the conductivity, i.e.,

$$\sigma = A\, e^{-B(1-\theta)^C} \qquad (8.)$$

where A is the conductivity of the oxidized phase, θ is the state of charge and B and C arc constants characterizing the change in the conductivity of Ni electrode during discharge. The gradient of protons through the active material is used to calculate the conductivity at each point, and the resistance across the film thickness is expressed as an integral. Application of Ohms's law across the solid phase yields:

$$\phi_{Ohmic} = \frac{(J_{Ni,\beta\beta} + J_{O_2,\beta\beta})\, L^2\, \rho_{\beta\beta}}{\varepsilon_{Ni} - \varepsilon_{ox\,\beta}} \qquad (9.)$$

Similar expressions have been used for both the α-γ and β-β phases. Since, the two phases arc assumed to be situated parallel to each other along the electrode surface, the effective film resistance and transfer current arc parallel combinations of individual [illegible] be mass transport of protons thr

Schottky Barrier Potential

At the Ni electrode the Ni substrate current collector is separated from hydroxide/oxy hydroxide active material by a semi-conducting barrier termed as Schottky layer.[14] A junction potential, termed as Schottky junction potential, is thus created at the tI)clal/metal oxide interface. The Schottky junction potential consists of a relaxation term to control the on-sol of the overpotential during charge/disch arge and a second term quantifying the overpotential as shown below:

$$\phi_{Junction} = \phi_{Substrate} - \left(1 - exp^{\int_{t_0}^{t_n} I_{cell} * Eff)\, dt}\right) * Scale * Tanh\,(I_{cell} * kT / Thk1) + Scale * Bias \qquad (1\,0.)$$

11 is assumed here, as a first approximation, that the Schottky junction characteristics of both α-γ and β-β phases arc identical, as may be expected from the identical values foı their (electronic) conductivities in the oxidized as well as reduced state. A single Schottky layer thus separates the Ni substrate from the active material in α-γ and β-β phases.

Mass balance

The general expression for the mass balance of a species in the electrolyte is

$$n_i = \frac{\sum_{ij}^{x} J_i}{n_j F} + D_i \nabla C_i \qquad (10)$$

where the first term is the consumption/generation of C_i due to electrochemical reaction, J_j, the second corresponds to the diffusion of the species due to concentration gradient ∇C_i (D_i is the diffusion coefficient) and the third term describes the transport through migration under a potential gradient of $\nabla \phi_{Solution}$ (Z_i is the charge and u_i is the mobility). Specific Equations for the mass balance Of h ydroxide ions, oxygen and proton arc

$$THK1 * \frac{dC_{OH}}{dt} = -THK1 \frac{(J_{Ni,\beta\beta} + J_{Ni,\alpha\gamma} + J_{o_2,\beta\beta}\, J_{o_2,\alpha\gamma})}{f} + D_{OH} * \frac{dC_{OH}}{THK2} \qquad (11)$$

$$THK1 * \frac{dC_{O_2,pro}}{dt} = -THK1 \frac{(J_{O_2,\beta\beta} J_{O_2,\alpha\gamma})}{f} + D_{O_2} * \frac{dC_{O_2,pro}}{THK2} \quad (12)$$

and

$$C_{H_{\beta\beta}} = \left(\frac{Length^2}{f D_H C_{Ni} (\varepsilon_{sub\,Ni_{\beta\beta}} - \varepsilon_{0\,Ni}) * (1 - E)_{0\,\beta\beta}) * (1 - \%\gamma)} \right) * B_{co\,eff,\beta\beta} * J_{Ni\,\beta\beta} - \text{Curr Sum} \quad (13)$$

respectively. The B coefficients are numerically evaluated parameters as described earlier.[6] Similar expressions have been used for the mass balance of the proton in the α-γ phase as Well.

Electrochemical kinetics

'1 'he kinetics of electrochemical process are governed by Butler-Volmer equation which is generally expressed as :

$$i_j = i_{0,j,0} \left[\exp\left(\frac{\alpha_{aj} F}{R T} \eta_j\right) - \exp\left(-\frac{\alpha_{cj} F}{R T} \eta_j\right) \right] \quad (14)$$

where the overpotential is given by:

$$\eta_j = \phi_s - \phi_l - U_{j,0} \quad (15)$$

and the exchange current density is given by:

$$i_{0,j,0} = i_{0,j,ref} \prod_i \left(\frac{a_{i,j}}{a_{i,ref}}\right)^{\gamma_{ij}} \quad (16)$$

Expressing the reversible potential in terms of 0, the mole fraction of reduced NiOOH (or concentration of proton):

$$\phi_{eq} = \phi^0_{eq} + \frac{RT}{nF} \ln\left(\frac{\theta}{1-\theta}\right) + \frac{RT}{nF} \ln\left(\frac{a_{OH^-}}{a_{H_2O}}\right) + K(\theta - 1) \quad (17)$$

The last term in the above equation is incorporated to explain the non-Nernstian behavior in the intercalation potentials of proton in nickel oxides. " In other words, it is an empirical fit to the observed electrode potential.

incorporation equations (15), (16) and (17) into equation (14) gives the expression for the electrokinetics of the redox reactions involving Ni oxides as :

$$J_{Ni,\beta\beta} = 2\,a_{max,1}\,I_{0,1,\beta\beta}\left[\left(\frac{C_{OH,1}}{C_{OH,Ref}}\right)\left(C_{H^+,\beta\beta,Surf}(1-\theta_{0,\beta\beta})e^{\frac{\alpha_{c,1}}{RT}f(\phi_{Ni,Sub}-\phi_{f,1}-\phi_{H^+,Ref})}\right)-\left(1-\left(C_{H^+,\beta\beta,Surf}(1-\theta_{0,\beta\beta})\right)e^{\frac{\alpha_{a,1}}{RT}f(\phi_{Ni,Sub}-\phi_{f,1}-\phi_{H^+,Ref})}\right)\right] \quad (18)$$

and

$$J_{Ni,\alpha\gamma} = 2\,a_{max,1}\,I_{0,1,\alpha\gamma}\left[\left(\frac{C_{OH,1}}{C_{OH,Ref}}\right)\left(C_{H^+,\alpha\gamma,Surf}(1-\theta_{0,\alpha\gamma})e^{\frac{-\alpha_{c,1}}{RT}f(\phi_{Ni,Sub}-\phi_{f,1}-\phi_{H^+,Ref})}\right)-\left(1-\left(C_{H^+,\alpha\gamma,Surf}(1-\theta_{0,\alpha\gamma})\right)e^{\frac{\alpha_{a,1}}{RT}f(\phi_{Ni,Sub}-\phi_{f,1}-\phi_{H^+,Ref})}\right)\right] \quad (19)$$

The corresponding equations for oxygen and hydrogen reactions arc:

$$J_{O,\beta\beta} = a_{max,1}\,I_{0,\beta\beta}\left[\left(\frac{C_{O_2}C_{OH}^{2}}{C_{OH,ref}^{2}}\right)e^{\frac{\alpha_{c,O_2}}{RT}f(\phi_{\beta\beta}-\phi_{f,1}-\phi_{O_2,ref})}-\left(\frac{C_{O_2}}{C_{O_2,ref}}\right)e^{\frac{\alpha_{a,O_2}}{RT}f(\phi_{\beta\beta}-\phi_{f,1}-\phi_{O_2,ref})}\right] \quad (20.)$$

and

$$J_{H_2,Ni} = a_{max,1}\,I_{0,H_2,Ni}\left[\left(\frac{C_{OH}}{C_{OH,ref}}\right)^{2\alpha_{c,H_2}}\left(\frac{P_{H_2}}{P_{H_2,ref}}\right)^{(\cosh(C_{OH}-C_{OH,ref})^{\gamma_{c,H_2}})}\left(e^{\frac{-\alpha_{c,O_2}}{RT}f(\phi_{c}-\phi_{f,1}-\phi_{H_2})}-e^{\frac{-\alpha_{a,O_2}}{RT}f(\phi_{c}-\phi_{f,1}-\phi_{H_2})}\right)\right] \quad (21.)$$

Similar expressions have been used to describe the reactions of gaseous species at both the α-γ and β-β phases. The rate of the electrochemical conversion of β-NiOOH into γ-NiOOH on overcharge is expressed as:

$$J_{H^+,\beta\gamma} = 2\,a_{max,1}\,I_{0,1,\beta\gamma}\left[C_{H^+,\beta\beta,Surf}(1-\theta_{0,\beta\beta})e^{\frac{-\alpha_{c,1}}{RT}f(\phi_{Ni,Sub}-\phi_{f,1}-\phi_{\beta\beta,Ref})}-1\right] \quad (22.)$$

The above is unidirectional; there is no conversion of the gamma phase to the beta unless through the reduced form of α-Ni(OH)$_2$. Finally, the kinetics of the chemical conversion process of α-Ni(OH)$_2$ to β-Ni(OH)$_2$ arc expressed by a first order Arrhenius -type rate equation as:

$$RATE_{\alpha\beta} = K_{0,\alpha\beta} * X_{\gamma} * (H^+_{\alpha\gamma})_{surf} * (1-\theta_{0,\alpha\gamma}) * e^{\left(\left(\frac{1}{T}-\frac{1}{T_0}\right)*\frac{E_{\alpha\beta}}{R}\right)} \quad (23)$$

where X_{γ} is the phase fraction of the α-γ phase.

other Governing Equations

Other ancillary collations utilized in the model are

Current balance :

$$I_{cell} = THK1 * \sum_{J} J_{Ni,J} \qquad (24)$$

Gamma Phase Fraction Balance :

$$X_{\gamma} = X_{\gamma,0} + \int_{t_0}^{t_n} J_{Ni,\beta\gamma}\, dt - \int_{t_0}^{t_n} K_{\alpha\beta}\, dt \qquad (25)$$

State of charge :

$$SOC_i = SOC_{i,0} + \sum_{j} J_{Ni,J}\, dt * MW_i \;/\; (Loading * n * F * X_i \qquad (26)$$

Efficiency :

$$Eff_{Ni} = \sum_{j} J_{Ni} \;/\; I_{cell} \qquad (27)$$

RESULTS

Discharge behavior of Ni-Cd and Ni-H_2 cells

Simulations have **been** performed with the above two-phase model under discharge and charge conditions. Figs. 3 and 4 shows the discharge curves of Ni-Cd and Ni-H_2 cells from models compared with the experimental data. These simulations were carried out with a marginally slower kinetics for the α-γ couple compared to the β-β couple (~80 and 200" μA/cm^2, respectively). The rest of the mode] parameters in the model arc described in our earlier publication.[14] As is clear from the figures, the agreement between the experimental data and the simulations has significantly improved, upon the incorporation of the second couple at the Ni electrode.

Charging

Regarding the charge process, it has been observed from our testing of a 50 Ah Eagle Picher, aerospace Ni-H_2 cell that at low temperatures (≤ -20°C), the charge profile consists of an additional plateau, before the roll-over (Fig. 3). This may be attributed to the conversion of β-NiOOH to γ-NiOOH, which is not as prominent at higher temperatures due to tile interfering oxygen evolution reaction. Wc have demonstrated this trend with simulations, using the two-phase model (Fig.4). The individual partial-current densities under these conditions, i.e.., corresponding to the main reaction and oxygen evolution at both the phases, β-NiOOH to γ-NiOOH conversion and α- Ni(OH)$_2$ to β-

$Ni(OH)_2$ transformation support the above deduction. Apparently, the kinetics of oxygen evolution process are relatively sluggish such that the electrochemical conversion of β-NiOOH to γ-NiOOH is facilitate at low temperatures. This would result in an increase in the capacity of the Ni-112 cell, due to a higher specific capacity of γ-NiOOH.

Cyclic Voltammetry

Finally, in an effort to further validate the two phase reaction scheme, the existing models of the nickel electrode were modified to simulate cyclic voltammetric behavior, by solving for the current at a time-dependent voltage. Any form of voltage sweep such as linear, triangular etc. can be adopted, with selected scan rates and number of cycles, Fig. 5 shows the typical cyclic voltammogram obtained from the model. Studies are underway to corroborate these voltammograms with experimental observations, especially under conditions favorable to both the phases.

CONCLUSIONS

The model incorporating tbc multiple phases of the active material at the Ni electrode in Ni rechargeable cells provides simulations with improved accuracy and c.loser to the experimental data, especially under favorable conditions such as extensive cycling, overcharge and low temperature charging. The reaction scheme include.s two redox couples of β-NiOOH/β-$Ni(OH)_2$ and y- NiOOH/α-$Ni(OH)_2$, an electrochemical, unidirectional conversion of β-NiOOH to γ-NiOOH and a chemical transformation of /α-$Ni(OH)_2$ to β-$Ni(OH)_2$.

ACKNOWLEDGMENTS

'l-his work was carried out at the Jet Propulsion Laboratory, California Institute of Technology, under contract with tile National Aeronautics and Space Administration and was sponsored by Code AE, Office of NASA's Chief Engineer's office.

REFERENCES

1. D. Fan and R. 11. White, *J. Electrochem. Soc.*, 138, 17 (1991).
2. D. Fan and R. E. White, J. *Electrochem. Soc.*, 138, 2952 (1991).
3. Z. Mao and R. E. White, *J. Electrochem. Soc.*, 138, 3354 (1991); *J. Electrochem. Soc.*, 141, 54 (1994).
4. P. De Vidts and R. E. White, *J. Electrochem. Soc.*, 142, 1509 (1995).

5. J. Newman and W. 11. Tiedeman, *AIC h E Journal*, 2 1 , 25 (1975); *Ind. and Engineering Chemistry Fundamentals, 367-369* (1978).
6. J. Weidner and P. Timmerman, *J. Electrochem. Soc.*, 141, 346 **(1994).**
7. I). Timmerman, S. Di Stefano, 1'. R. Gluck and 1). E. Perrone, *Proc. 26th IECEC* , 358,(1991).
8. H. Bode, K. Dehmelt and J. Witte, *Electrochim. Acta*, 11, 1079 (1966).
9. A. Delahaye-Vidal et al, ECS Proceedings, Vol. 90-4, p 58 (1990).
10. A. Zimmerman, ECS Proceedings, Vol. 94-7, **p.** 268 **(1** 994).
I 1. R. Barnard, C. F. Randel and F. L. Tye, *J. Appl. Electrochem.*, 10, 109 (1980).
12. **R.** A. 1 Iuggins, H. Prinz, M. Wohlfahrt-Meherens, L. Jorissen and W. Witschel, *Solid State Ionics*, 70/7 1,417 (1 994).
13. Z. Mao, 1'. De Vidts, R. E. White and J. Newman, *J. Electroche m. Soc.*, **1 4 1 , 54** (1994).
I **4.11.** V. Ratnakumar, P. Timmerman, C. Sanchez, S. Di Stefano and G. 1 Ialpert, *J. Electrochem. Soc.* , *143,* 803 (1996).
15. R. Barnard, C. F. Randel and **1:. 1,.** Tye, *J. Appl. Electrochem.*, 10, 109 (1980).

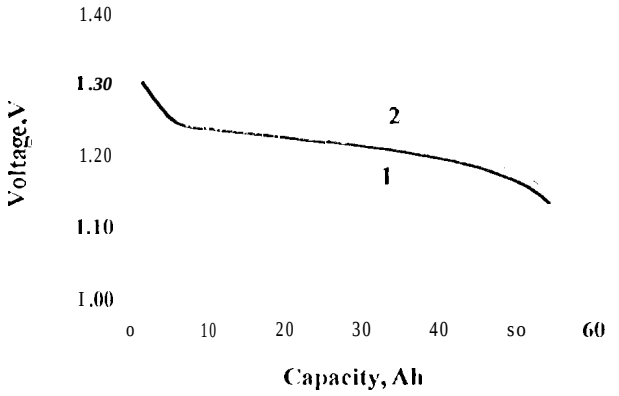

Fig. 1 : Comparison of 1) simulated discharge curve (bold line) of a 50 Ah TOPEX cell with ?) experimental data (dashed line) at C/2 and 25°C.

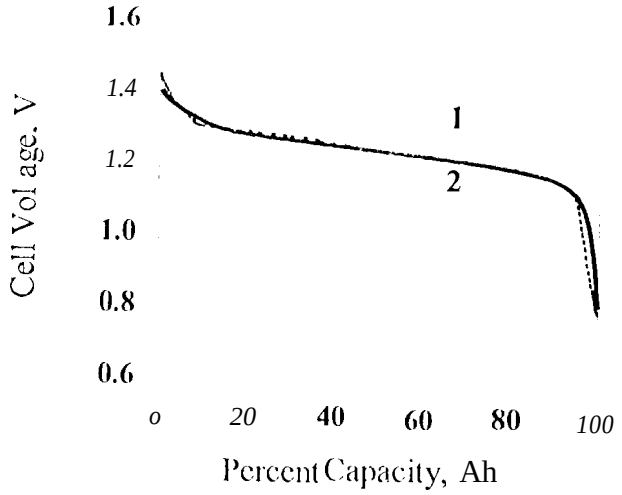

Fig. 2: Comparison of 1) simulated discharge curve (bold line) of a 5(I Ah EPI cell with 2) experimental data (dashed line) at C/2 and 25°C.

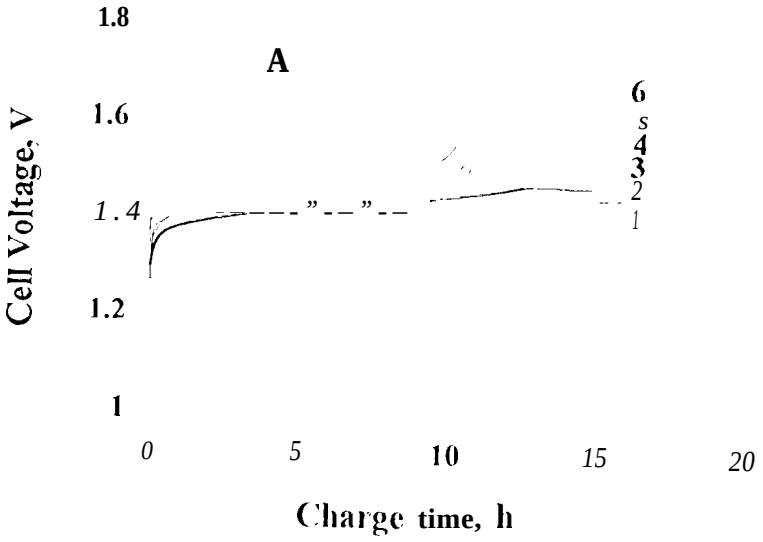

Fig. 3: Experimental charge curves of a Ni-111 ccl] at C/10 and at various temperatures of I) 35, 2) 20, 3) 10, 4) 0, and 5) -10 and 6) -2(I "(', respectively.

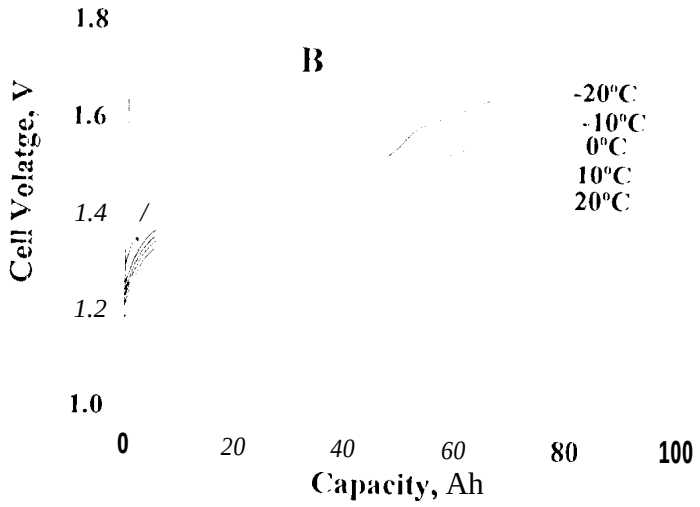

Fig. 4: Simulated charge curves of a Ni-H_2 cell at C/10 and at various temperatures.

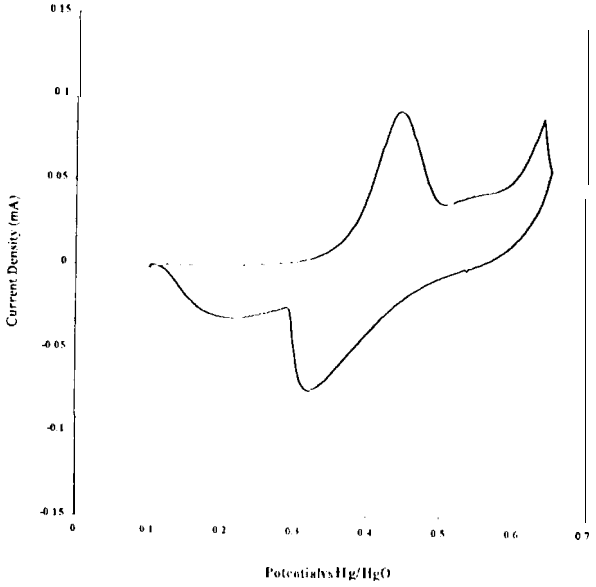

Fig. 5: Typical simulated DC cyclic voltammetric curve of Ni oxide electrode in 7 M KOH.